AD-A169 856 PLASMA JOINING OF METAL MATRIX COMPOSITES(U) MSNW INC 1/1
SAN MARCOS CA G H REYNOLDS ET AL. FEB 86
ARO-22817.2-MS-S DAAG29-85-C-0027

UNCLASSIFIED F/G 11/4 NL

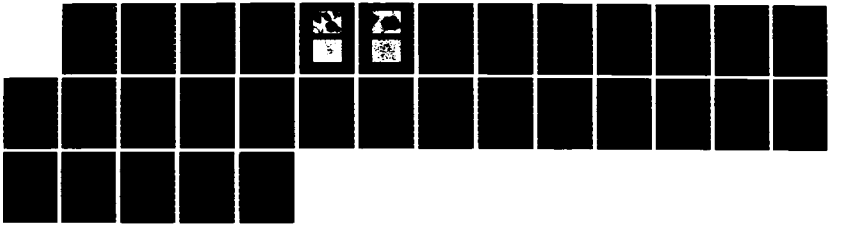

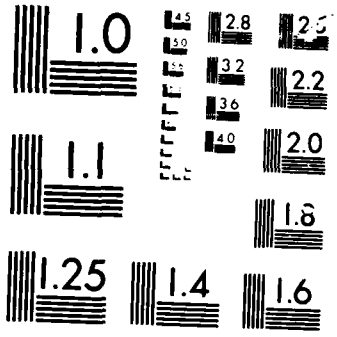

MSNW, INC.

P.O. Box 865
San Marcos, California 92069
(619) 744-7648

PLASMA JOINING OF METAL MATRIX COMPOSITES

Submitted to U.S. Army Research Office

Contract No. DAAG29-85-C-0027

Interim Technical Report - December 1985/January 1986

Prepared By:
G.H. Reynolds and L. Yang, MSNW, Inc.

UNCLASSIFIED

SECURITY CLASSIFICATION OF THIS PAGE (When Data Entered)

REPORT DOCUMENTATION PAGE		READ INSTRUCTIONS BEFORE COMPLETING FORM
1. REPORT NUMBER ARO 22817.2-MS-S	2. GOVT ACCESSION NO. AD-A161056 N/A	3. RECIPIENT'S CATALOG NUMBER N/A
4. TITLE (and Subtitle) PLASMA JOINING OF METAL MATRIX COMPOSITES		5. TYPE OF REPORT & PERIOD COVERED Interim Technical December 1985/January 1986 6. PERFORMING ORG. REPORT NUMBER N.A.
7. AUTHOR(s) G.H. REYNOLDS AND L. YANG		8. CONTRACT OR GRANT NUMBER(s) DAAG29-85-C-0027
9. PERFORMING ORGANIZATION NAME AND ADDRESS MSNW, Inc. P.O. Box 865 San Marcos, CA 92069		10. PROGRAM ELEMENT, PROJECT, TASK AREA & WORK UNIT NUMBERS
11. CONTROLLING OFFICE NAME AND ADDRESS U. S. Army Research Office Post Office Box 12211 Research Triangle Park, NC 27709		12. REPORT DATE February 1986 13. NUMBER OF PAGES 27
14. MONITORING AGENCY NAME & ADDRESS(if different from Controlling Office)		15. SECURITY CLASS. (of this report) Unclassified 15a. DECLASSIFICATION/DOWNGRADING SCHEDULE

16. DISTRIBUTION STATEMENT (of this Report)

Approved for public release; distribution unlimited.

17. DISTRIBUTION STATEMENT (of the abstract entered in Block 20, if different from Report)

NA

18. SUPPLEMENTARY NOTES

The view, opinions, and/or findings contained in this report are those of the author(s) and should not be construed as an official Department of the Army position, policy, or decision, unless so designated by other documentation.

19. KEY WORDS (Continue on reverse side if necessary and identify by block number)

Composite materials, joining, plasma processing, thermochemistry.

20. ABSTRACT (Continue on reverse side if necessary and identify by block number)

Microstructural details of the first 1100 Al/SiC and Al(Zr)/SiC precomposited powders are described. These powders will be used for initial low pressure plasma depositions. Modeling of expected bulk and interfacial reactions and degradation mechanisms in plasma processing of the composite powder filler metals is described in detail.

DD FORM 1 JAN 73 1473 EDITION OF 1 NOV 65 IS OBSOLETE

UNCLASSIFIED

SECURITY CLASSIFICATION OF THIS PAGE (When Data Entered)

ABSTRACT

Microstructural details of the first 1100 Al/SiC and Al(Zr)/SiC precomposited powders are described. These powders will be used for initial low pressure plasma depositions. Modeling of expected bulk and interfacial reactions and degradation mechanisms in plasma processing of the composite powder filler metals is described in detail.

COMPOSITE POWDER PREPARATION

Precomposited powders were prepared from 1100 aluminum (commercial purity) and aluminum - 3.0 wt.% Zr inert gas atomized powders with a dispersed SiC particulate reinforcing phase. Each composite powder composition contained 25 wt.% of the SiC particulate reinforcing phase. Although the uniformity of dispersion of the reinforcing phase is not yet completely satisfactory and experimentation is continuing to produce composite powders suitable for initial plasma deposition trials, preliminary findings are described herein.

Figure 1a. shows an optical micrograph at 500X magnification of the microstructure of cross sections of 1100 aluminum/SiC precomposited powder particles. The macroscopic uniformity of dispersion of the reinforcing phase throughout the volume of the composite powder particle is apparent. Particle-to-particle uniformity is not yet completely satisfactory. Figure 1b. shows a scanning electron micrograph of a composite particle cross section at 5000X where the SiC dispersion in the aluminum alloy matrix is more easily seen.

Figures 2a. and 2b. show analogous cross sectional optical and scanning electron micrographs of precomposited powders prepared with an aluminum - 3.0 wt.% Zr alloy matrix and 25 wt.% SiC particulate reinforcing phase.

When a sufficiently uniform dispersion of the SiC phase in the aluminum

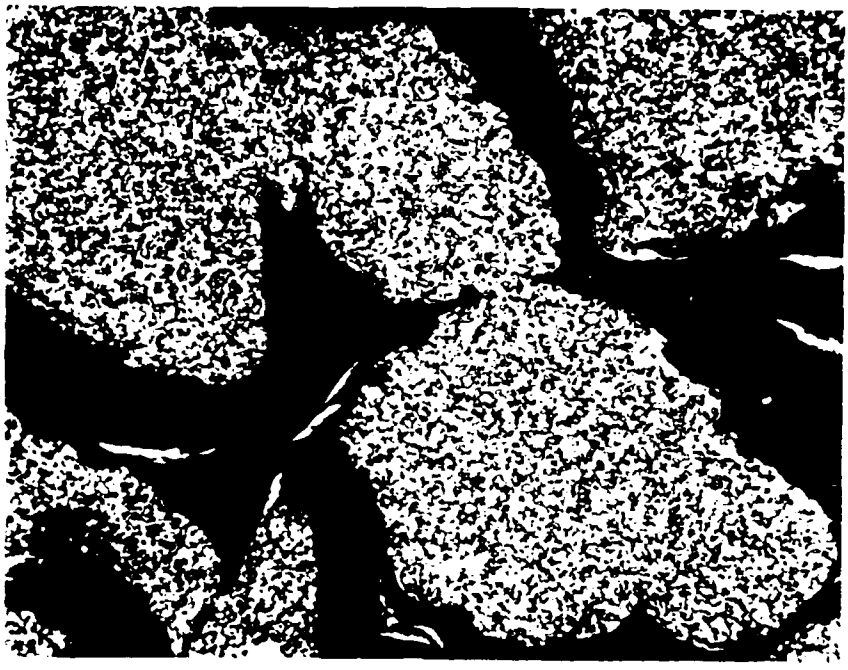

Figure 1a. Cross Sections of 1100 Aluminum/SiC.
Precomposited Powders. Magnification (500X)

Figure 1b. Cross Section of 1100 Aluminum/SiC.
Precomposited Powder. Scanning Electron Micrograph.
Magnification (5000X)

Figure 2a. Cross Sections of Aluminum - 3.0 wt.% Zr/SiC. Precomposited Powders. Magnification (500X)

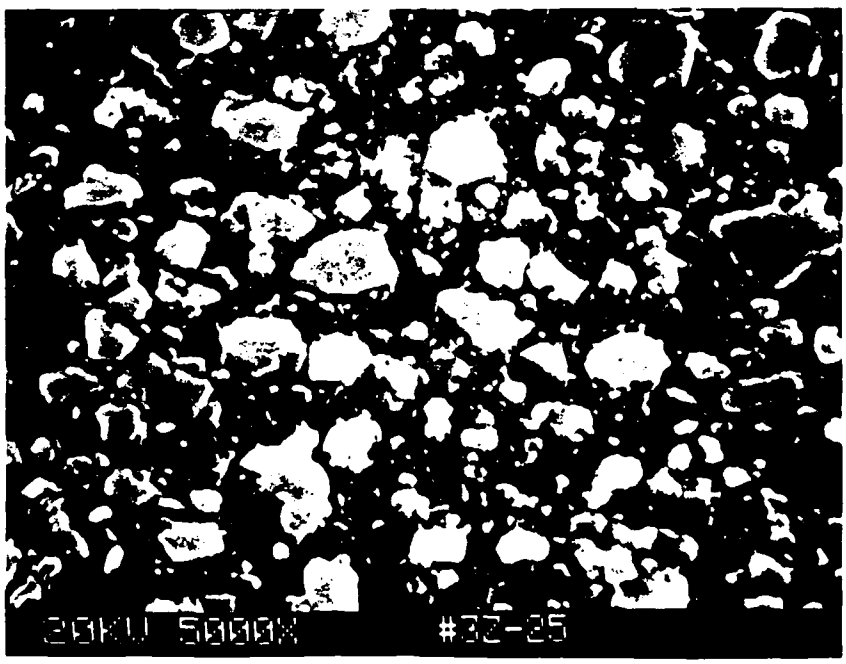

Figure 2b. Cross Section of Aluminum - 3.0 wt.% Zr/SiC. Precomposited Powder. Scanning Electron Micrograph. Magnification (5000X)

alloy matrices has been achieved, these materials will be produced in pound quantities and characterized in detail, particularly for bulk and localized compositions, prior to low pressure plasma processing. Comparison of actual plasma processing effects to theoretically predicted effects can then be made.

ANALYTICAL STUDIES

Thermodynamic and kinetic analyses of the physical and chemical events occuring during plasma processing of composite powders, which may affect the structure and properties of the deposit, were continued during this reporting period. Preliminary results obtained are described below:

1. Reaction Between the Liquid Al Matrix and the SiC Dispersion.

(1). Reaction between liquid Al and SiC to form Al_4C_3.

The reaction under consideration is:

$$3\ SiC\ (s) + 4\ Al\ (l) \rightarrow Al_4C_3\ (s) + 3\ Si\ \text{(dissolved in liquid Al)} \qquad (1)$$

The equilibrium activity of Si dissolved in liquid Al, a^*_{Si}, for this reaction was calculated from the standard free energy of reaction ΔF^o obtained from the literature (Reference (1)) by using the equation

$$\Delta F^o = - RT \ln a^*_{Si} = - 13.714\ T \log a^*_{Si} \qquad (2)$$

over the temperature range 1000-2300°K. The results are shown in Table 1.

a^*_{Si} represents the Si activity at the interface between the liquid Al and the SiC dispersion when they are in equilibrium. Reaction (1) will proceed only if the Si formed at the interface is removed continuously by diffusion into the bulk of the liquid Al matrix, and the $Al_4C_3(s)$ formed is not a barrier for Si, Al and C transport.

Assume a composite model consisting of alternate layers of SiC and liquid Al of 10^{-3} cm thickness each, with the Si activity at the interface equal to a^*_{Si}. The average Si activity , $\bar{a}_{Si}$, in the liquid Al layer after a diffusion time of t seconds can be represented by the equation (Reference (2)):

$$R = \frac{\bar{a}_{Si}}{a^*_{Si}} = 1 - \frac{8}{\pi^2} \sum_{n=0}^{\infty} \frac{1}{(2n+1)^2} \exp\left[-\left(\frac{(2n+1)\pi}{10^{-3}}\right)^2 Dt\right] \qquad (3)$$

where R is defined as the degree of saturation, since when R=1, i.e. $\bar{a}_{Si} = a^*_{Si}$, the reaction will stop, and D = diffusion constant for Si in liquid Al. Equation (3) shows that R is a function of Dt. R values for Dt = $10^{-6}, 10^{-7}, 10^{-8}$, and 10^{-9} cm^2 were calculated using Equation (3). These Dt values were selected because the D values for diffusion in liquid metal systems are usually in the range of 10^{-5} to 10^{-4} cm^2/sec (Reference (3)), and the residence time for the composite powder in the plasma is expected to be in the range of 10^{-4} to 10^{-2} second. The calculated R values are given in Table 2.

The depletion of the SiC dispersed phase inventory by Reaction (1) can be calculated as follows. The total number of Si atoms present in the liquid Al

Table 1

Equilibrium Si Activity, a^*_{Si}, for Reaction (1). at Various Temperatures

Temperature (^oK)	a^*_{Si}
1000	0.226
1100	0.200
1200	0.180
1300	0.165
1400	0.152
1500	0.142
1600	0.135
1700	0.128
1800	0.122
1900	0.118
2000	0.113
2100	0.110
2200	0.107
2300	0.104

Table 2

Degree of Saturation for Si in Liquid Al for Various Dt Values

Dt (cm^2)	Degree of Saturation (R)
10^{-6}	1
10^{-7}	0.698
10^{-8}	0.229
10^{-9}	0.075

layer of 10^{-3}cm thickness and 1 cm^2 cross sectional area, n_{Si}, is related to the average molefraction $\bar{N}_{Si}$ of Si in this liquid Al layer by the equation:

$$\bar{N}_{Si} = \frac{n_{Si}}{n_{Si} + n_{Al}} \tag{4}$$

where n_{Al} = number of Al atoms in the liquid Al layer of 10^{-3} cm thickness and 1 cm^2 cross sectional area = $\frac{1cm^2 \times 10^{-3}cm \times 2.7\ gm./c.c.}{27\ gm/mole}$

$\times\ 6.1 \times 10^{23}$ atoms/mole = 6.1×10^{19}

If the solution of Si in Al can be considered as an ideal solution, then $\bar{N}_{Si} = \bar{a}_{Si}$ and from Equation (4)

$$n_{Si} = \frac{\bar{a}^*_{Si}}{1 - \bar{a}_{Si}} \times 6.1 \times 10^{19} = \frac{R\, a^*_{Si}}{1 - R\, a^*_{Si}} \times 6.1 \times 10^{19} \tag{5}$$

The total number of Si atoms in the SiC layer of 10^{-3} cm thickness and 1 cm^2 cross sectional area is

$$\frac{10^{-3}cm \times 1\ cm^2 \times 3.2\ gm/c.c.}{40\ gm/mole} \times 6.1\ 10^{23}\ atoms/mole = 4.88 \times 10^{19}.$$

From Equation (5), the fractional depletion F for the SiC inventory is:

$$F = \frac{n_{Si}}{4.88 \times 10^{19}} = 1.25\ \frac{R\, a^*_{Si}}{1 - Ra^*_{Si}} \tag{6}$$

Equation (6) can be used to calculate the loss of the SiC dispersed phase

due to reaction with the liquid Al matrix to form Al_4C_3 during plasma processing of the composite powders as a function of temperature and time if the D values for the diffusion of Si in liquid Al at these temperatures are known. Estimates can be made by assuming a D value of 10^{-5} cm^2/sec. at 1000^oK and an activation energy for diffusion, Q, of 8000 calories/mole. These assumptions may not be unreasonable considering the diffusion data for liquid metal systems reviewed in Reference (3).

Using $D_{1000\ ^oK} = 10^{-5}$ cm^2/sec. and Q = 8000 calories/mole, the D value for 2300^oK was found to be about 10^{-4} cm^2/sec. Using these D values, the R and F values for t = 10^{-2}, 10^{-3}, and 10^{-3}second were calculated from Equation (3) and Equation (6), respectively. The results are shown in Table 3.

It is interesting to note that the depletion of SiC is less at 2300^oK than at 1000^oK for t = 10^{-2} second. This is due to the fact that the liquid Al becomes saturated with Si before t = 10^{-2}seconds is reached and that the Si activity at saturation is lower at 2300^oK than at $1000\ ^oK$ (0.104 versus 0.226), since Al_4C_3 is l ; stable at higher temperatures. It is also interesting to see that the F values for the same t values are relatively insensitive to temperature. The loss of SiC can be held to about a few percent if t 10^{-4} seconds, about several percent if t 10^{-3}second, and about twenty percent if t 10^{-2}second, for both T = 1000^oK and T = 2300^oK.

(2). Other possible reactions.

Since Al_4C_3 is unstable at high temperatures, as indicated by the decrease of the a^*_{Si} value with the increasing temperature (see Table 1), the following reaction which does not involve the formation of Al_4C_3, was considered.

Table 3

Depletion of SiC Dispersed Phase by Reaction with Liquid Al Matrix to Form Al_4C_3

$T(^oK)$	$D(cm^2/sec)$	a^*_{Si}	t(seconds)	R	F
1000	10^{-5}	0.226	10^{-2}	0.698	0.234
			10^{-3}	0.229	0.068
			10^{-4}	0.075	0.022
2300	10^{-4}	0.104	10^{-2}	1	0.145
			10^{-3}	0.698	0.098
			10^{-4}	0.229	0.030

$$SiC\ (s) \rightarrow C\ (s) + Si\ (\text{in liquid Al}) \qquad (7)$$

For this reaction, $\Delta F^{o} = - Rt \ln a^{*}_{Si}$. The a^{*}_{Si} values for 1000, 1500, 2000, and 2300°K were calculated by using thermodynamic data from the literature (Reference (1)). The results are shown in Table 4.

These a^{*}_{Si} values are much smaller than that for Reaction (1) at the same temperature (see Table 1), suggesting that Reaction (1), not Reaction (7), is favored for the temperature range shown in Tables 1 and 4.

2. Reaction Between the Alloying Elements and the SiC Dispersion.

(1) Reaction between Zr dissolved in liquid Al and SiC.

The reaction under consideration is:

$$SiC\ (s) + Zr\ (\text{in liquid Al}) \rightarrow ZrC\ (s) + Si\ (\text{in liquid Al}) \qquad (8)$$

The equilibrium activities of Zr and Si in liquid Al, a^{*}_{Zr} and a^{*}_{Si}, are related to the standard free energy of the reaction, ΔF^{o} by the equation.

$$\Delta F^{o} = -RT \ln \frac{a^{*}_{Si}}{a^{*}_{Zr}} = - 4.571\ T \log \frac{a^{*}_{Si}}{a^{*}_{Zr}} \qquad (9)$$

Table 4

Equilibrium Si Activity for Reaction (7)

$T^{o}K$	a^{*}_{Si}
1000	3.83×10^{-4}
1500	7.12×10^{-3}
2000	0.031
2300	0.054

Using thermodynamic data available in the literature (Reference (1)), the values of a^*_{Si}/a^*_{Zr} were calculated for the temperature range 1000-2300°K. These calculated values are shown in Table 5. Included in the same table are the a^*_{Zr} values in equilibrium with the a^*_{Si} values given in Table 1 for each of the temperatures indicated in these tables. These are the a^*_{Zr} values needed to maintain the equilibrium a^*_{Si} values high enough to stop Reaction (1). The results in Table 5 show that the a^*_{Si}/a^*_{Zr} values are extremely high, implying that Reaction (8) is highly favored. They also show that the a^*_{Zr} values needed to stop Reaction (1) are much lower than that corresponding to the lowest concentration of Zr (0.5 wt. %) in the Al alloy matrix to be used in this program. If the solution of Zr in liquid Al can be considered as ideal, the a_{Zr} for the 0.5 wt. % alloy is 1.49×10^{-3}.

The above analysis shows that it is possible to use Zr additions to the liquid Al matrix to prevent liquid Al from reacting with SiC to form Al_4C_3 since Zr reacts preferentially with SiC rather than Al. The Si formed according to Equation (8), if its activity in the liquid Al is increased to a value higher than the equilibrium Si activity for Reaction (1), can prevent Reaction (1) from happening. However, for the Zr-Al alloy matrix materials used in this program, the Zr concentration is not high enough to accomplish this goal. Even for the alloy containing 3 wt. % Zr, the highest activity of Si attained after all the Zr has reacted with SiC is only 0.009 which is much lower than the equilibrium Si activity.

Use of Al alloys of higher Zr concentration to overcome this problem is undesirable, since this involves the loss of a significant amount of SiC in order to increase the activity of Si in the Al to the value needed. In fact, a better approach would be to prealloy the required amount of Si to the Al matrix. However, the effect of large additions of Si to the Al on the

Table 5

Thermodynamic Evaluation of Reaction (8)

$T^{o}K$	a^{*}_{Si}/a^{*}_{Zr}	a^{*}_{Zr} Needed to Prevent Reaction(1)
1000	2.31×10^{6}	9.78×10^{-8}
1100	6.08×10^{5}	3.28×10^{-7}
1200	1.95×10^{5}	9.21×10^{-7}
1300	7.37×10^{4}	2.23×10^{-6}
1400	3.20×10^{4}	4.75×10^{-6}
1500	1.55×10^{4}	9.16×10^{-6}
1600	9.11×10^{3}	1.48×10^{-5}
1700	4.69×10^{3}	2.73×10^{-5}
1800	2.85×10^{3}	4.28×10^{-5}
1900	1.82×10^{3}	6.48×10^{-5}
2000	1.22×10^{3}	9.26×10^{-5}
2100	8.52×10^{2}	1.29×10^{-4}
2200	6.12×10^{2}	1.75×10^{-4}
2300	4.53×10^{2}	2.30×10^{-4}

mechanical properties of the matrix of the composite would have to be carefully considered.

Addition of a small amount (e.g. 0.5-3 wt. %) of Zr to the Al may prevent the reaction of Al with SiC by another mechanism. As shown by the data in Table 5, the SiC reacts preferentially with the Zr rather than the Al to form a layer of ZrC over the SiC surface, which may act as a barrier to protect the SiC from being attacked by the Al. ZrC is stable toward Al. This can be shown by considering the reaction:

$$3\ ZrC\ (s) + 4\ Al\ (\ell) \rightarrow Al_4C_3(s) + 3\ Zr\ (\text{in liquid Al}) \qquad (10)$$

and calculating the equilibrium activity of Zr in liquid Al, a^*_{Zr}, using the standard free energy of the reaction ΔF^o, according to the equation:

$$\Delta F^o = -\ RT\ \ln\ (a^*_{Zr})^3 = -\ 13.714\ T\ \log\ a^*_{Zr} \qquad (11)$$

The calculated a^*_{Zr} values for 1000-2300°K are given in Table 6. It can be seen that these a^*_{Zr} values are very small, implying that Reaction (10) is not favored and ZrC is very stable toward Al(1) at the temperatures indicated in Table 6.

The thickness of the ZrC layer required for it to be protective must be determined experimentally. The maximum thickness of the ZrC layer which can be formed from the Zr in the two Zr-Al alloys (0.5 and 3 wt. % Zr) used as matrix materials in this program can be calculated by considering a model composite consisting of alternate layers of SiC and liquid Zr-Al alloy of 10^{-3}cm

Table 6

Thermodynamic Evaluation of the Reaction Between ZrC and Al(1)

$T^{o}K$	a^{*}_{Zr}
1000	9.77×10^{-8}
1100	3.29×10^{-7}
1200	9.22×10^{-7}
1300	2.23×10^{-6}
1400	4.77×10^{-6}
1500	9.19×10^{-6}
1600	1.65×10^{-5}
1700	2.72×10^{-5}
1800	4.30×10^{-5}
1900	6.48×10^{-5}
2000	9.30×10^{-5}
2100	1.29×10^{-4}
2200	1.75×10^{-4}
2300	2.29×10^{-4}

thickness each. For the 0.5 wt. % Zr-Al alloy, the maximum thickness of the ZrC layer which can be formed on the SiC surface on each side of the liquid Zr-Al alloy layer is 1.14×10^{-6} cm. For the 3 wt. % Zr-Al alloy, this thickness is 6.84×10^{-6}cm.

The actual thickness of ZrC formed on the SiC surface during plasma processing can be calculated on the basis of the model composite described above assuming that the rate-determining factor for the growth of the ZrC layer is the transport of Zr from the bulk of the liquid alloy layer to the SiC surface and that the activity of Zr is zero at the SiC surface. The average activity of Zr in the liquid alloy layer, $\bar{a}_{Zr}$, is related to the residence time in the plasma, t, by the equation (Reference (2)):

$$\frac{\bar{a}_{Zr}}{a^{o}_{Zr}} = \frac{8}{\pi^2} \sum_{n=0}^{\infty} \frac{1}{(2n+1)^2} \exp\left[-\left(\frac{(2n+1)\pi}{10^{-3}}\right)^2 Dt\right] \qquad (12)$$

where D = diffusion constant for Zr in liquid Al at the plasma temperature,

a^{o}_{Zr} = initial activity of Zr in the liquid alloy layer,

= 9.09×10^{-3} for the alloy containing 3.0 wt. % Zr,

and 1.49×10^{-3} for the alloy containing 0.5 wt. % Zr.

The fractional depletion of the Zr inventory in the liquid alloy layer, F_d, after time t in the plasma is:

$$F_d = \frac{a^{o}_{Zr} - \bar{a}_{Zr}}{a^{o}_{Zr}} = 1 - \frac{8}{\pi^2} \sum_{n=0}^{\infty} \frac{1}{(2n+1)^2} \exp\left[-\left(\frac{(2n+1)\pi}{10^{-3}}\right)^2 Dt\right] \qquad (13)$$

The F_d and $\bar{a}_{Zr}$ values for Dt = 10^{-6}, 10^{-7}, 10^{-8} and 10^{-9} cm^2 were calculated, using Equation (13), for the two alloys (0.5 wt. % and 3.0 wt. % Zr) used in this program. The results are shown in Table 7.

Included in Table 7 are also the losses of Zr atoms, Δn_{Zr}, from the liquid alloy layer (10^{-3} cm thick, 1 cm^2 cross sectional area) by diffusion to the SiC surface to form ZrC. Δn_{Zr} was calculated from the equation:

$$\Delta n_{Zr} = n^o_{Zr} - n_{Zr} = n^o_{Zr} - \frac{\bar{a}_{Zr}}{1-\bar{a}_{Zr}} \times n_{Al} \qquad (14)$$

where n^o_{Zr} = number of Zr atoms in the liquid alloy layer of 10^{-3} cm thickness and 1 cm^2 cross sectional area

$$= \frac{10^{-3}\text{cm} \times 1\ \text{cm}^2 \times 2.7\ \text{gm/c.c.} \times (\text{wt. \% Zr})}{91.22\ \text{gm/mole} \times 100} \times 6.1 \times 10^{23}$$

$= 9.028 \times 10^{16}$ for 0.5 wt. % Zr alloy and

5.417×10^{17} for 3.0 wt. % Zr alloy

n_{Zr} = number of Zr atoms in the same liquid alloy layer after loss by diffusion

$$= \frac{\bar{a}_{Zr}}{1 - \bar{a}_{Zr}} \cdot n_{Al}$$ if the solution of Zr in Al is ideal (see Eq. 5)

n_{Al} = number of Al atoms in the same liquid alloy layer

$$= \frac{10^{-3}\ \text{cm} \times 1\ \text{cm}^2 \times 2.7\ \text{gm/c.c.} \times (\text{wt. \% Al})}{27\ \text{gm/mole} \times 100} \times 6.1 \times 10^{23}$$

$= 6.070 \times 10^{19}$ for 0.5 wt. % alloy and

5.917×10^{19} for 3.0 wt. % alloy

The thickness of ZrC formed on the SiC surface can be calculated from Δn_{Zr}

Table 7

Loss of Zr Atoms from Liquid Zr-Al Alloys by Diffusion to the Surface of SiC to Form ZrC

$Dt(cm^2)$	F_d	a_{Zr}		Δn_{Zr}	
		0.5 wt.% Zr*	3.0 wt.% Zr**	0.5 wt.% Zr	3.0 wt.% Zr
10^{-6}	1.0	0	0	9.028×10^{16}	5.417×10^{17}
10^{-7}	0.698	4.50×10^{-4}	2.75×10^{-3}	6.297×10^{16}	3.790×10^{17}
10^{-8}	0.229	1.15×10^{-3}	7.01×10^{-3}	2.048×10^{16}	1.269×10^{17}
10^{-9}	0.075	1.38×10^{-3}	8.41×10^{-3}	6.521×10^{15}	4.408×10^{16}

*$a^{o}_{Zr} = 1.49 \times 10^{-3}$

**$a^{o}_{Zr} = 9.09 \times 10^{-3}$

as a function of time in the plasma if the D values for the diffusion of Zr in liquid Al at the plasma temperature are known. Assuming D = 10^{-5} cm^2/sec. at 1000°K and 10^{-4} cm^2/sec. at 2300°K, the thickness of ZrC formed on the SiC surface at these temperatures for t = 10^{-2}, 10^{-3}, and 10^{-4} seconds was calculated for the two Zr-Al alloys (0.5 wt. % and 3.0 wt. % Zr) used in this program, using 6.73 gm/c.c. as the density of ZrC. The results are shown in Table 8.

It can be seen that the thickness of ZrC formed on the SiC surface is very thin. Whether such thin ZrC layers can protect SiC from reaction with Al during plasma processing must be determined experimentally.

(2) Reaction between Ti dissolved in Liquid Al and SiC.

The results for Ti-Al alloy matrix are expected to be similar to that for Zr-Al alloy matrix. No analytical calculations were performed.

(3) Reaction between B dissolved in Liquid Al and SiC.

The reaction to be considered is:

$$SiC\ (s) + 4\ B\ (\text{in liquid Al}) \rightarrow B_4C\ (s) + Si\ (\text{in liquid Al}) \qquad (15)$$

The ratio of the equilibrium activities of B and Si in liquid Al, a^*_B and a^*_{Si}, can be calculated from the standard free energy of reaction, ΔF^o, obtained from thermodynamic data in Reference (1), by the equation:

$$\Delta F^o = - RT \ln \left(\frac{a^*_{Si}}{a^{*4}_B} \right) = - 4.317\ T \log \left(\frac{a^*_{Si}}{a^{*4}_B} \right) \qquad (16)$$

Table 8

Thickness of ZrC Formed on SiC Surface at 1000 and 2300°K as a Function of Time in Plasma

T°K	D(cm^2/Sec)	t(seconds)	Thickness of ZrC on SiC (cm)	
			0.5 wt.% Zr Alloy	3.0 wt.% Zr Alloy
1000	10^{-5}	10^{-2}	7.92×10^{-7}	4.76×10^{-6}
		10^{-3}	2.57×10^{-7}	1.60×10^{-6}
		10^{-4}	8.20×10^{-8}	1.11×10^{-6}
2300	10^{-4}	10^{-2}	1.14×10^{-6}	6.84×10^{-6}
		10^{-3}	7.92×10^{-7}	4.76×10^{-6}
		10^{-4}	2.52×10^{-7}	1.60×10^{-6}

The calculated results for the temperature range 1000 - 2300°K are shown in Table 9. The small values of a^*_{Si}/a^{*4}_{B} indicate that Reaction (15) is not favored.

Further thermodynamic analysis of the reaction

$$3\ B_4C\ (s) + 4\ Al\ (l) \rightarrow Al_4C_3\ (s) + 12\ B\ (\text{in liquid Al}) \qquad (17)$$

shows that any B_4C formed is not stable in liquid Al. The equilibrium activities of B, a^*_B, for the temperature range 1000 - 2300°K, were calculated from the standard free energy of reaction, ΔF^o, according to the equation:

$$\Delta F^o = -\ RT\ \ln a_B^{*12} = -\ 54.85\ T\ \log a_B^* \qquad (18)$$

The calculated results are shown in Table 10. The a^*_B values obtained are larger than or comparable with the a^*_{Si} values for the SiC-Al reaction at the same temperature (see Table 1). This indicates that B_4C is not stable in liquid Al at the temperatures indicated in Table 10. The addition of B to the Al matrix therefore cannot prevent the reaction between SiC and Al during plasma processing.

3. Removal of Hydrogen from Molten Al Alloy Droplets in Plasma

In the interim technical report for October/November 1985, the fractional loss of the hydrogen in the Al alloy matrix during its residence time, t, in

Table 9

Thermodynamic Evaluation of B and SiC in Liquid Al

$T(^{o}K)$	a^{*}_{Si}/a^{*4}_{B}
1000	0.032
1200	0.060
1400	0.092
1600	0.126
1800	0.160
2000	0.195
2200	0.228
2300	0.245

Table 10

Thermodynamic Analysis of the Reaction Between B_4C and Al

$T(^{o}K)$	a^{*}_{B}
1000	1.63
1200	1.32
1400	1.13
1600	1.02
1800	0.44
2000	0.20
2200	0.10
2300	0.08

the plasma was calculated for t = 10^{-2}, 10^{-3} and 10^{-4} seconds, assuming the Al alloy to be at its melting point and using a diffusion constant D = 7.6 x 10^{-4} cm^2/sec for hydrogen in liquid Al at its melting point. Similar calculations were carried out during this reporting period for a temperature of 1258°K, using a D value of 5.6 x 10^{-3} cm^2/sec given in Reference (4). All the calculated results, together with those given in the October/November 1985 interim report are shown in Table 11. It can be seen that if the oxide film on the droplets does not impede the removal of hydrogen from the droplet surface, a large fraction of the hydrogen in the droplets will be lost in the plasma if the residence time is longer than 10^{-3} second.

4. Summary of Analytical Results

Analytical results for the major physical and chemical events occuring in the plasma can be summarized as follows:

1. Loss of Al matrix material by evaporation is less than 10% even at 2300°K if the residence time in plasma is less than 10^{-3}second.
2. Losses of (1) Zr, Ti and B alloying elements, (2) SiC, ZrC, and TiC dispersion, and (3) Al_2O_3 film on Al matrix, are negligible at 2300°K for in-plasma residence times as long as 10^{-2} second.
3. Significant amounts of hydrogen dissolved in the Al matrix are lost at the melting point of Al if the residence time in plasma is longer than 10^{-3} second and the presence of an oxide film on the surface of the molten droplets does not impede the removal of hydrogen from droplet surface.
4. SiC will react with the Al matrix to form Al_4C_3. Loss of SiC by such reaction is about 10% at 2300°K for in-plasma residence time of 10^{-3} second, if the rate limiting factor is the diffusion of the Si produced into the molten Al.

Table 11

Removal of Hydrogen From Molten Al Alloy Droplets in Plasma

Radius of Molten Al Alloy Droplets (cm)	Residence Time In Plasma (sec.)	Fractional Removal of Hydrogen From Droplets	
		$933^{o}K$	$1258^{o}K$
75×10^{-4}	10^{-2}	0.84	1.00
	10^{-3}	0.35	0.77
	10^{-4}	0.12	0.31
22×10^{-4}	10^{-2}	1.00	1.00
	10^{-3}	0.87	1.00
	10^{-4}	0.38	0.81

5. Zr and Ti alloying additions will react with SiC to form ZrC and TiC, which are stable toward Al. For the highest Zr and Ti alloy concentrations used in this program (3 wt. % Zr and 5 wt. % Ti), the maximum thickness of ZrC and TiC formed in a model composite, containing alternate layers of SiC and Al of 10 microns thickness each, are 0.07 micron and 0.17 micron respectively.
6. B alloying additions do not prevent the reaction between SiC and Al. B_4C is not as stable toward Al as ZrC and TiC.

These predecitions will be compared with the results obtained on the compositions and microstructures of the Al-SiC, Al(Zr)-SiC, Al(Ti)-SiC and Al(B)-SiC feed materials and that of the plasma deposits on inert water-cooled copper substrates at various power levels and distances between the nozzle and the substrate as a prelude to plasma joining of metal matrix composites.

REFERENCES

(1) JANAF Thermochemical Tables, Second Edition, July, 1970

(2) Diffusion in Solids, Liquids, and Gases, by W.Jost, Academic Press, New York, 1952

(3) L. Yang and G. Derge, "General Consideration of Diffusion in Melts of Metallurgical Interest", Proceedings of Metallurgical Society Conferences, Volume 7, Physical Chemistry of Process Metallurgy, Part 1, p. 503.

(4) A. Vashchenko, et al, Isvest. Met. 15, No. 1, pp. 50-56 (1972)

END

DTIC

7-86